

Kicking massive black holes off clusters: Intermediate-mass ratio inspirals

Symeon Konstantinidis^{1,2*}, Pau Amaro-Seoane^{2,3**} & Kostas D. Kokkotas^{4,5***}

¹ Astronomisches Rechen-Institut, Mönchhofstraße 12-14, 69120, Zentrum für Astronomie, Universität Heidelberg, Germany

² Max Planck Institut für Gravitationsphysik (Albert-Einstein-Institut), D-14476 Potsdam, Germany

³ Institut de Ciències de l'Espai (CSIC-IEEC), Campus UAB, Torre C-5, parells, 2^{na} planta, ES-08193, Bellaterra, Barcelona, Spain

⁴ Theoretical Astrophysics (TAT), IAAT, Eberhard Karls University of Tübingen, Auf der Morgenstelle 10, 72076 Tübingen, Germany

⁵ Department of Physics, Aristotle University of Thessaloniki, Thessaloniki 54124 Greece

May 18, 2012

ABSTRACT

Context. Contrary to supermassive and stellar-mass black holes (SBHs), the existence of intermediate-mass black holes (IMBHs) with masses ranging between $10^{2-4} M_{\odot}$ has not yet been confirmed. The main problem in the detection is that the innermost stellar kinematics of globular clusters (GCs), the natural loci to IMBHs, are very difficult to resolve. However, if IMBHs reside in the centre of GCs, a possibility is that they interact dynamically with their environment. A binary formed with the IMBH and a compact object of the GC would naturally lead to a prominent source of gravitational radiation, detectable with future observatories.

Aims. We use N -body simulations to study the evolution of GCs containing an IMBH and calculate the gravitational radiation emitted from dynamically formed IMBH-SBH binaries and the possibility that the IMBH escapes the GC after an IMBH-SBH merger.

Methods. We run for the first time direct-summation integrations of GCs with an IMBH including the dynamical evolution of the IMBH with the stellar system and relativistic effects, such as energy loss in gravitational waves (GWs) and periastris shift, and gravitational recoil.

Results. We find in one of our models an intermediate-mass ratio inspiral (IMRI), which leads to a merger with a recoiling velocity higher than the escape velocity of the GC. The GWs emitted fall in the range of frequencies that a LISA-like observatory could detect, like the European eLISA or in mission options considered in the recent preliminary mission study conducted in China. The merger has an impact on the global dynamics of the cluster, as an important heating source is removed when the merged system leaves the GC. The detection of one IMRI would constitute a test of GR, as well as an irrefutable proof of the existence of IMBHs.

Key words. (Galaxy:) globular clusters: general - gravitational waves - Methods: numerical - Stars: kinematics and dynamics

1. Motivation

IMBHs possibly exist in the centres of GCs with masses between $M \sim 10^{2-4} M_{\odot}$, if we assume that they follow the observed correlations between supermassive BHs and their stellar surroundings (see Miller & Colbert 2004; Miller 2009, and references therein). Nonetheless, we do not have a clear detection of an IMBH, although there are favouring evidences that suggest that they should exist. In particular, the work of Farrell et al. (2009, 2012) derive a conservative lower limit of $500 M_{\odot}$ for an IMBH in the edge-on spiral galaxy ESO243-49 based on the variability of a X-ray source which has a maximum $0.2 - 10$ keV luminosity of up to $1.1 \times 10^{42} \text{ erg s}^{-1}$. Other recent interesting observational examples that point to the existence of these objects are the work of Sutton et al. (2012), which evaluates a sample

of eight extreme luminosity ultra-luminous X-ray source candidates and state that the observed luminosities can be explained in terms of IMBHs with masses in the range of $10^3 - 10^4 M_{\odot}$. Nyland et al. (2012) present Expanded Very Large Array observations of the dwarf lenticular galaxy NGC 404 and find that the most likely scenario is an accreting IMBH, ruling out other scenarios based on the observed X-ray and/or radio luminosities.

Contrary to our Galactic Centre, we cannot use current observational techniques to detect a massive black hole in a GC. The radius of influence of an IMBH is of a few arc seconds (Peebles 1972; Chanamé et al. 2010; Miller & Colbert 2004). For instance, for a $10^4 M_{\odot}$ IMBH, the influence radius is of $\sim 5''$ assuming a central velocity dispersion of $\sigma = 20 \text{ km s}^{-1}$ and a distance of $\sim 5 \text{ kpc}$ (see also Miller & Colbert 2004, for a similar example).

There are other uncertainties, such as the availability of a bright reference star, which make the case rather improbable. Hence, we would need the Very Large Telescope inter-

* e-mail: Simos@ari.uni-heidelberg.de

** e-mail: Pau.Amaro-Seoane@aei.mpg.de

*** e-mail: Kostas.Kokkotas@uni-tuebingen.de

ferometer and one of the next-generation instruments, the VSI or GRAVITY (Gillessen et al. 2006; Eisenhauer et al. 2008). In that case we could improve the astrometric accuracy by an order of magnitude and thus we would possibly be in the position of detecting the innermost kinematics of a GC around a potential IMBH. An interesting avenue towards the *direct* detection of an IMBH is GW astronomy. Additionally, these systems represent an excellent test of GR, since they are similar to extreme-mass ratio inspirals (Amaro-Seoane et al. 2007). In particular, space-borne detectors such as the ESA-led eLISA (Amaro-Seoane et al. 2012) or Chinese mission study options (“ALIA” from now onwards, see Bender et al. 2005; Crowder & Cornish 2005; Gong et al. 2011) will be able to catch these systems with good signal-to-noise ratios (SNR) if the GC is not further than $z \sim 0.7$ (Amaro-Seoane et al. 2012).

2. Numerical tool and initial conditions

We integrate the dynamical evolution of a globular cluster with *Myriad* (Konstantinidis & Kokkotas 2010), a direct-summation N -body code that integrates all gravitational forces for all particles at every time step. The programme uses the Hermite integration scheme (Aarseth 1999, 2003). This requires computation of not only the accelerations, but also their time derivatives. Particles that are tightly bound or with very small separation are integrated using the time-symmetric Hermite scheme (Kokubo et al. 1998), which is a symplectic integrator that makes the numerical errors oscillate between two limits that can be controlled by the choice of the time step. The code uses post-Newtonian correcting terms to the Newtonian forces, including 1, 2 and 2.5 order, as described for the first time in an N -body code by Kupi et al. (2006) (their equations 1, 2 and 3), as well as a recipe for gravitational recoil. The recoil velocity depends strongly on the mass ratio of the two holes, on the magnitude of their spins and on their directions with respect to the plane of the orbit (see e.g. Rezzolla 2009, and references therein). The equation that we have implemented in the code is taken from Lousto et al. (2010),

$$\mathbf{v} = (v_m + v_\perp \cos \xi) \hat{e}_1 + v_\perp \sin \xi \hat{e}_2 + v_\parallel \hat{e}_3. \quad (1)$$

In the last equation, the indices \perp and \parallel stand for perpendicular and parallel directions with respect to the orbital angular momentum vector \mathbf{L} of the binary. \hat{e}_1 is a unit vector and lies on the plane of the orbit connecting the two MBHs, with direction from the heavier to the lighter one. \hat{e}_2 is also on the plane of the orbit, but perpendicular to \hat{e}_1 , with direction such that \hat{e}_1 , \hat{e}_2 and \hat{e}_3 construct an orthonormal system, with \hat{e}_3 defined such that it is the unit vector parallel to \mathbf{L} . ξ is the angle between the unequal contributions of mass and spin to the recoil velocity. We assign random, maximal spins to the stars of the GC, and in particular we initially give the IMBH a spin $a = S/M^2$ (see e.g. Lousto et al. 2010) of 0.998.

The number and masses of SBHs are of particular importance in our simulations. For this reason we created a large number of initial data for star clusters and evolved the stars using the stellar evolution code *sse* (Hurley et al. 2000). We used Kroupa-like initial mass functions (IMF, see Kroupa 2001) with different values for the slopes α_1 (slope for $m \leq 0.5M_\odot$) and α_2 (slope for $m > 0.5M_\odot$). We

fixed the total number of stars to $N = 32768$, the lower stellar mass limit to $m_{\text{low}} = 0.2M_\odot$ and the upper mass limit to $m_{\text{upper}} = 150M_\odot$. Finally, we used values for the metallicity Z ranging from 0.0001 to 0.02. For each model we created 100 sets of initial data and evolved the stars for 10 Myr, because this is the time in which all of the most massive stellar-mass BHs, the ones that could interact strongly and have an impact on the IMBH, form. In our models we assumed no supernova kicks, so that all SBHs formed are retained in the cluster. The number of SBHs depends strongly on the choice of the IMF and ranges from ~ 20 to ~ 70 in our models. On the other hand the masses of the SBHs depend on the metallicity and range from $\sim 3M_\odot$ (for $Z = 0.02$) to $\sim 27M_\odot$ (for $Z < 0.001$).

Since it is not possible to dynamically evolve all the initial data sets we created, we picked 4 representative cases that produce low and high numbers of SBHs. We also picked a value $Z = 0.001$ for the metallicity as typical for a GC which resulted in the formation of SBHs with masses between $\sim 13M_\odot$ and $27M_\odot$. In those models all stars with masses above $20M_\odot$ have evolved off the main sequence at 10 Myr.

For our fiducial simulation A we choose slopes $\alpha_1 = 1.3$ and $\alpha_2 = 2.4$, which results in 62 stellar-mass BHs in the system. For the distribution of stars and BHs in the cluster we use a King profile (King 1966) with concentration parameter $W_0 = 7$. The escape velocity at the centre of the clusters is $\sim 17\text{ km s}^{-1}$. No primordial mass segregation is taken into account, so the BHs formed in all the distances from the centre of the cluster. The absence of initial mass-segregation leads to an underestimate in the number of compact objects that will interact with the IMBH. The sizes of a star or a stellar remnant are taken into account only in the case of collisions. At the centre of the cluster we introduce an IMBH of mass $M_\bullet = 500M_\odot$ and correct the velocities of all stars and BHs of the GC to reach dynamical equilibrium.

We run also three additional simulations with different parameters. Case B is like A but with $M_\bullet = 1,000M_\odot$ and $\alpha_2 = 2.5$, which results in 52 SBHs; case C is like B but with a King parameter of 6 and 48 SBHs, and D is like A but with a King parameter of 6 and $\alpha_1 = 1.2$ and $\alpha_2 = 2.7$, which result in 17 SBHs. Nevertheless, only case A had an IMRI; we will therefore in the remainder of the article focus on this case. In all simulations we turned off further stellar evolution, which, if turned-on, would form more SBHs in the GC. This is a simplification, which does not have a significant impact on the dynamics of the IMBH and therefore on our results, since the low-mass SBHs that would form if stellar evolution was turned-on, would have a negligible influence on the IMBH, even if they merge with it.

3. Dynamics of the system

Initially, the IMBH interacts strongly with a sub-group of stars and BHs that contains approximately 20 members. As the system evolves, the members of this sub-group change. Soon, most of the stellar-mass BHs of the system sink towards the centre and start to interact with the IMBH and its environment. During this process, some of them receive big kicks due to 3-body interactions and are slingshot away from the centre of the cluster or GC itself. After $T \sim 3$ Myr the first stable IMBH-SBH binary forms. The companion of

the IMBH is a SBH with mass $m_{\bullet,11} = 23.9 M_{\odot}$ and the initial semi-major axis of this binary is $a \sim 88$ AU. At $T \sim 9.2$ Myr this binary has a strong interaction with another SBH of the system. The interaction leads to a change of companion for the IMBH, which now builds a binary with a SBH of mass $m_{\bullet,18} = 20.1 M_{\odot}$. The initial semi-major axis of the new binary is $a \sim 17.6$ AU. This binary survives for nearly 40 Myr, but its characteristics vary significantly. At $T \sim 49$ Myr the semi-major axis changes to $a \sim 5$ AU, while the eccentricity increases to $e = 0.965$. At this point in the simulation, this binary interacts strongly with the second most massive SBH, which leads to a companion exchange. The new binary has an initial semi-major axis of $a \sim 6.55$ AU and a very high eccentricity, of $e = 0.999$. The mass of the new companion SBH is $m_{\bullet,2} = 26.54 M_{\odot}$. In Fig.(1) we show the evolution of the semi-major axis and eccentricity for all of these binaries combined into a single curve. After some $T \sim 13,000$ yr the binary merges and the resulting IMBH receives a random recoil velocity that depends on the mass ratio of the two members of the system and on the random spins that the code assigned to them. This “gravitational rocket” or recoil is such that the resulting velocity exceeds the escaping velocity and the merged system leaves the GC. This is due to the fact that we are using a low number of stars for the clusters; more realistic clusters will have larger escape velocities, so that the retained fraction of recoiling IMBH is larger and not well-represented by our case. We studied the distribution of recoil velocities for a merger of a binary similar to that of simulation A. We ran a two-body interaction 10^7 times and calculated the recoil using equation 1 with different spin orientations and magnitudes for the two black holes. We found that the most probable recoil velocity for a binary such as the one of case A peaks around 25 km s^{-1} , with a probability of 21% that the merged system achieves velocities greater than 50 km s^{-1} , of the order of realistic escape velocities.

In Fig. (2) we show the evolution of the distances of the 10 most massive SBHs from the center. The SBHs inspiral the center very rapidly, as long as the IMBH exists in the cluster. Some of them escape the system, after passing very close to the central binary. After the IMBH merges with its binary companion SBH, the coalesced system leaves the GC and the trajectories of the remaining SBHs are not as steep, because they orbit the center of density of the GC without sinking rapidly into it. In Fig. (3) we show the Lagrange radii of the cluster during the simulation. We stop the simulation at ~ 10 Myr after the ejection of the IMBH. The Lagrange radii increase instantly when the merged system leaves the system, but they start decreasing slowly shortly after that. This decrease will probably lead to a new core collapse of the system unless some hard binaries are formed. The IMBH-SBH binary represented a heating source in the center of the GC, transferring kinetic energy to the stars and SBHs that passed close from the density center. The lack of the binary makes the system core and internal radii decrease in size unless another heating source is formed and stops the shrinkage of the GC. Even though we integrated the system for another ~ 10 Myr after the ejection, no such source formed.

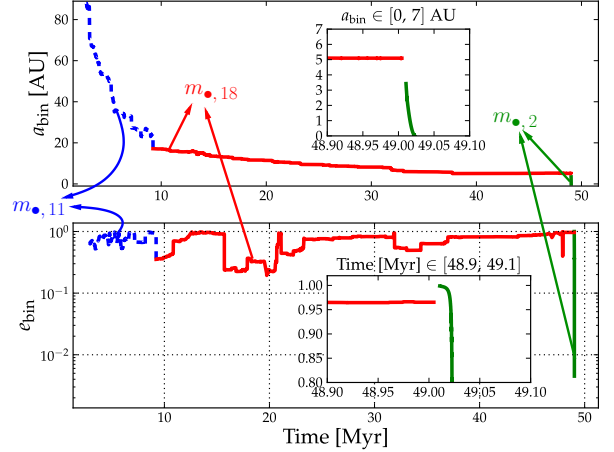


Fig. 1. Evolution of the semi-major axis and eccentricity of the different three binaries formed with the IMBH. Shortly after the beginning of the simulation, the IMBH builds a binary with the SBH with the 11th most massive mass, $m_{\bullet,11}$. This corresponds to the first part of the curve (dashed blue curve). Later there is an interaction which leads to a companion exchange for the binary, the SBH with the 18th most massive mass, $m_{\bullet,18}$. This binary lives for about 40 Myr. We can see that the two first binaries have phases of very high eccentricity, $e_{\text{bin}} \sim 1$, but not high enough to lead to a coalescence. The jumps in e_{bin} indicate that the IMBH-SBH is still in a regime in which interactions with other stars play an important role. The system shrinks further and further until there is a three-body interaction. The binary is unbound and for a short period of time the IMBH has no companion, as indicated in the zoom-in subplots embedded in both, the upper and lower panels. Then the final binary forms, with the second most massive SBH. This binary is very hard and quickly losses energy via GWs radiation, which very efficiently leads to circularization and the final merger.

4. Gravitational waves from an IMRI

In this section we follow the binary IMBH-SBH from the standpoint of emission of GWs. In Fig.(4) we can see the evolution of the IMRI in a semi-major axis and orbital period – eccentricity plane. The binary enters the plot from the top with a high eccentricity, which places it very close to the innermost stable circular orbit, but the loss of energy quickly circularises it and drives it to lower eccentricities. As we discussed in the previous section, the binary forms with a very small initial semi-major axis, so that it hardens very efficiently. Hence, the binary follows closely what we can expect from the approach of Peters (1964), since the post-Newtonian terms lead the evolution of the system, which can be regarded as dynamically decoupled from the GC. It then enters the band of a LISA-like or ALIA detector with a significant eccentricity and the simulation is stopped when the semi-major axis is $a = 5 R_{\text{Schw}}$, the Schwarzschild radius of the IMBH. That is the moment at which the code assigns a recoil velocity to the merged system based on the spins of the two compact objects.

In Fig.(5) we can see the same from the perspective of the characteristic amplitude and frequency of the waves.

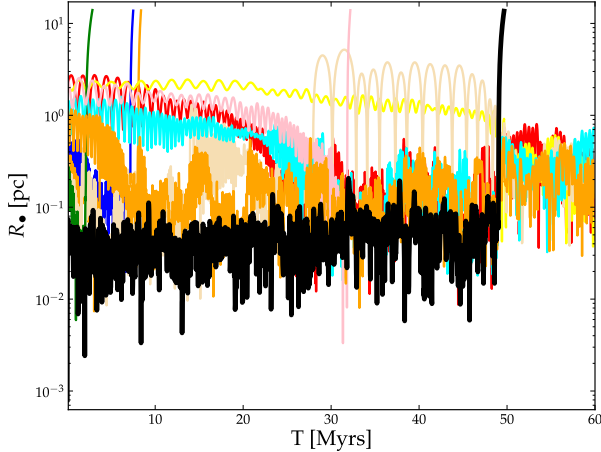


Fig. 2. Distance R_{\bullet} to the density center of the GC of the ten most massive SBHs and the IMBH (solid black line). Strong interactions of the SBHs lead to ejection of four of them before the IMBH merges. They are removed from the simulation when $R_{\bullet} > 10$ pc and they are unbound with the GC. At $T \sim 47.7$ Myr the IMRI leads to a coalescence that kicks the resulting merged system off the GC.

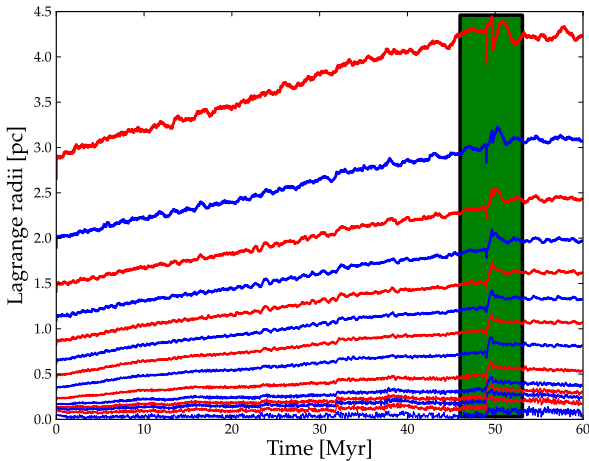


Fig. 3. Lagrangian radii showing the evolution of different mass fractions in the cluster: from the top to the bottom 90, 80 ... 20, 10, 5, 3, 2, 1 and 0.1% of the total mass. The green rectangle shows the interval of time before and after the kick of the IMBH off the cluster. All mass curves suffer a jump at the moment of ejection. After the removal of the heating source from the center, the curves are flatter and their slopes start to decrease.

We display the first harmonics in the approximation of Keplerian ellipses of Peters & Mathews (1963).

5. Conclusions

In this work we have investigated with a direct-summation code the evolution of GCs that harbours an IMBH in their center. The code uses relativistic corrections and a prescription for gravitational recoil. For one of the cases we find that an IMRI forms with a SBH due to close interactions,

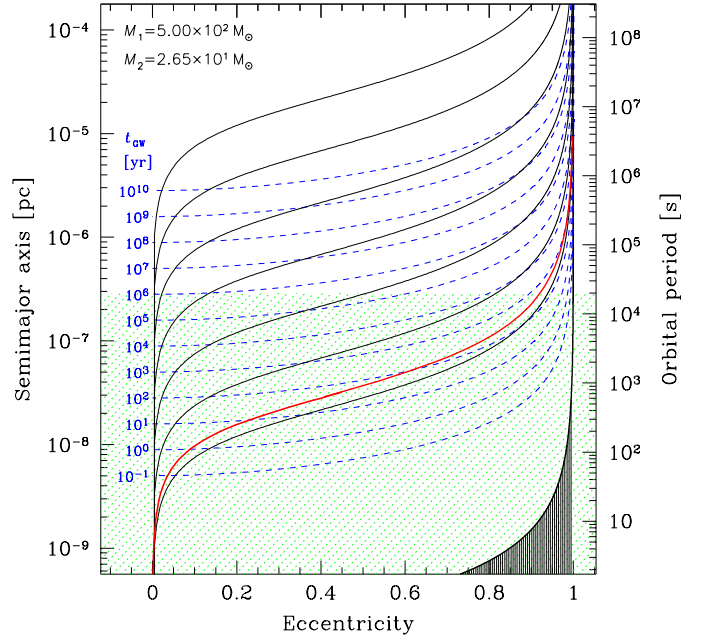


Fig. 4. Inspiral of the SBH into the IMBH from the top to the bottom and from the left to the right in the eccentricity–semi-major axis plane. The red, solid curve starting at a very eccentric orbit shows the results of the N-body simulation. The dashed, green region corresponds to the band of a LISA-like mission. Dashed, blue curves correspond to the trajectories due only to the emission of GWs in the Peters & Mathews (1963) approximation. We also plot the corresponding merger timescales in the same approximation in dashed, blue lines starting at 10^{10} years, and in solid, black lines the corresponding trajectories for evolution by GW emission Peters (1964) approximation. The black-shaded region on the right corresponds to the last stable circular orbit. Since the binary starts at a very high eccentricity, it basically follows one of the solid black lines, because it merges quickly and does not interact with other stars in the system.

which leads to the ejection of the binary after coalescence. We follow the properties of the IMRI from a standpoint of GWs and the global evolution of the cluster. For $z \leq 0.7$ the energy loss in GWs is easily detectable by space-borne missions such as a LISA-like observatory (Amaro-Seoane et al. 2012) or ALIA in its 8 pc configuration. Moreover, the IMRI enters the bandwidth of the detectors with a very high eccentricity, $e = 0.9987$, as with the EMRIs. One year before the final coalescence, the system still retains a residual eccentricity of $e \sim 0.12$, and ten minutes before merger of $e \sim 10^{-3}$, which is detectable by data-analysis techniques (Amaro-Seoane et al. 2010; Porter & Sesana 2010; Key & Cornish 2011).

IMRIs represent a test of GR, as well as a probe of space and time around massive black holes and also of the innermost kinematics of GCs to very large distances, of the order of a few Gpc. On the top of that, a successful detection would represent very robust proof for the existence of IMBHs. The fact that the kick is making the merged system leave the GC is possibly an artifact of the low particle number we used in the simulations, though in principle recoiling

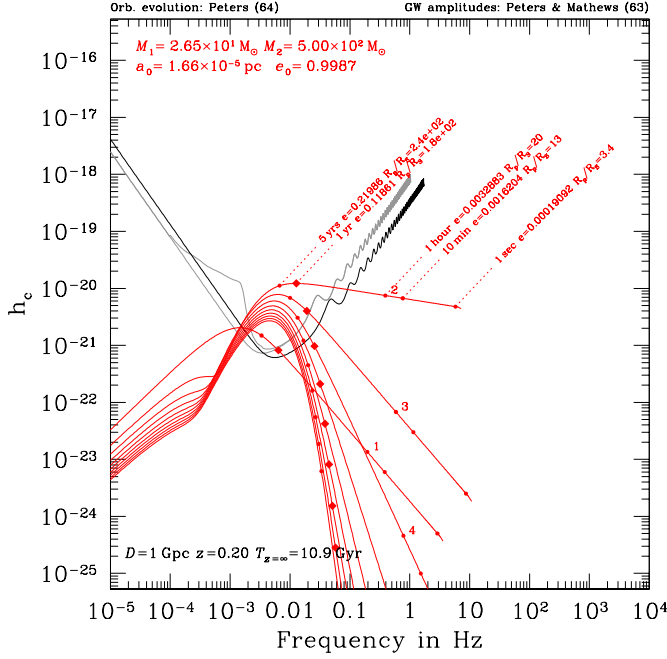


Fig. 5. Characteristic amplitude h_c of the first harmonics of the quadrupolar gravitational radiation emitted during the inspiral of the IMRI. The numbers show the first four of the harmonics. The orbital evolution is calculated in the Peters (1964) approximation and the amplitudes as in Peters & Mathews (1963). We assume the source is at a distance $D = 1$ Gpc. We indicate with a solid curve the noise curve $\sqrt{f} S_h(f)$ for the ALIA detector with an armlength of 3×10^9 m, a telescope diameter of 0.58 m, and a 1-way position noise of $8/\sqrt{\text{Hz}}$ pm; i.e. the 3H configuration of Xu, S., et al. (2011). We also add the noise curve for a LISA-like detector (in grey, Larson et al. 2000), with the Galactic binary white dwarf confusion background (Bender & Hils 1997). Note that the SNR is not given by the height above the curve, but by the area below it. For each panel we show the ratio R_p^0/R_s , the initial periaaps distance over the Schwarzschild radius of the system. We indicate the moments in the evolution for which the time to coalescence is 5, 1 yr, 1 hour, 10 minutes and 1 sec.

velocities can be much higher than the escape velocity of a cluster, of the order of $\sim 50 \text{ km s}^{-1}$ (see e.g. Rezzolla 2009; Holley-Bockelmann et al. 2008). However, we have also demonstrated that there is a non-negligible statistical probability that a similar case leads to a kick of the IMBH off a realistic GC. In spite of the code been ported to run on a PC with special-purpose hardware GRAPE, we can not cover a broader parameter space, nor study cases with a larger number of stars, or study the global dynamical evolution of the GC after the kick for a longer time. We plan on performing more accurate integrations on GPUs which will allow us to address the limitations we described above. This will allow us to investigate the potential global structure of the GC after the kick, since the impact on the cluster could in principle be a signature for the process.

Acknowledgements. We thank Emma Robinson for comments on the manuscript and Nikolaos Stergioulas for suggesting us to examine also the possibility of kicks. SK and PAS are indebted to Xuefei Gong, Shan Bai and Yun Kau Lau for conversations, their hospitality in

Beijing and for sharing with us the data for the sensitivity curve of the ALIA detector. PAS thanks the organizers of the 2011 summer workshop at the Aspen Center for Physics for inviting him to attend. SK and PAS are thankful to Rainer Spurzem and Fukun Liu for the invitation to the meeting in Lijiang on black holes and to visit the KIAA and NAOC in Beijing in summer of 2011, where this work was finished. The work of SK was funded by the Deutsches Zentrum für Luft- und Raumfahrt (DLR; through the LISA Germany project), also by the German Science Foundation (DFG) via SFB/TR7 on “Gravitational Waves” and by the German Academic Exchange Service (DAAD). SK would like to thank Kleomenis Tsiganis for discussions.

References

- Aarseth S. J., 1999, The Publications of the Astronomical Society of the Pacific, 111, 1333
- Aarseth S. J., 2003, Gravitational N-Body Simulations. ISBN 0521432723. Cambridge, UK: Cambridge University Press, November 2003.
- Amaro-Seoane P., Aoudia S., Babak S., Binétruy P., et. al 2012, ArXiv e-prints
- Amaro-Seoane P., Eichhorn C., Porter E. K., Spurzem R., 2010, MNRAS, 401, 2268
- Amaro-Seoane P., Gair J. R., Freitag M., Miller M. C., Mandel I., Cutler C. J., Babak S., 2007, Classical and Quantum Gravity, 24, 113
- Bender P. L., Armitage P. J., Begelman M. C., Perna R., 2005, White Paper submitted to the NASA SEU Roadmap Committee
- Bender P. L., Hils D., 1997, Classical and Quantum Gravity, 14, 1439
- Chanamé J., Bruursema J., Chandar R., Anderson J., van der Marel R., Ford H., 2010, in de Grijs R., Lépine J. R. D., eds, IAU Symposium Vol. 266 of IAU Symposium, HST’s hunt for intermediate-mass black holes in star clusters. pp 231–237
- Crowder J., Cornish N. J., 2005, Physical Review D, 72, 083005
- Eisenhauer F., Perrin G., Brandner W., Straubmeier C., et al. 2008, in Society of Photo-Optical Instrumentation Engineers (SPIE) Conference Series Vol. 7013 of Society of Photo-Optical Instrumentation Engineers (SPIE) Conference Series, GRAVITY: getting to the event horizon of Sgr A*
- Farrell S. A., Servillat M., Pforr J., Maccarone T. J., Knigge C., Godet O., Maraston C., Webb N. A., Barret D., Gosling A. J., Belmont R., Wiersema K., 2012, ApJ Lett., 747, L13
- Farrell S. A., Webb N. A., Barret D., Godet O., Rodrigues J. M., 2009, Nat, 460, 73
- Gillessen S., Perrin G., Brandner W., Straubmeier C., Eisenhauer F., Rabien S., Eckart A., Lena P., Genzel R., Paumard T., Hippler S., 2006, in Society of Photo-Optical Instrumentation Engineers (SPIE) Conference Series Vol. 6268 of Society of Photo-Optical Instrumentation Engineers (SPIE) Conference Series, GRAVITY: the adaptive-optics-assisted two-object beam combiner instrument for the VLTI
- Gong X., Xu S., Bai S., Cao Z., Chen G., Chen Y., He X., Heinzel G., Lau Y.-K., Liu C., Luo J., Luo Z., Pulido Patón A., Rüdiger A., Shao M., Spurzem R., Wang Y., Xu P., Yeh H.-C., Yuan Y., Zhou Z., 2011, Classical and Quantum Gravity, 28, 094012
- Holley-Bockelmann K., Gültekin K., Shoemaker D., Yunes N., 2008, ApJ, 686, 829
- Hurley J. R., Pols O. R., Tout C. A., 2000, MNRAS, 315, 543
- Key J. S., Cornish N. J., 2011, Phys Rev D, 83, 083001
- King I. R., 1966, AJ, 71, 64
- Kokubo E., Yoshinaga K., Makino J., 1998, MNRAS, 297, 1067
- Konstantinidis S., Kokkotas K. D., 2010, A&A, 522, A70+
- Kroupa P., 2001, MNRAS, 322, 231
- Kupi G., Amaro-Seoane P., Spurzem R., 2006, MNRAS, pp L77+
- Larson S. L., Hiscock W. A., Hellings R. W., 2000, Physical Review D, 62, 062001
- Lousto C. O., Campanelli M., Zlochower Y., Nakano H., 2010, Classical and Quantum Gravity, 27, 114006
- Miller M. C., 2009, Classical and Quantum Gravity, 26, 094031
- Miller M. C., Colbert E. J. M., 2004, International Journal of Modern Physics D, 13, 1
- Nyland K., Marvil J., Wrobel J., Young L., Zauderer B. A., 2012, ArXiv e-prints
- Peebles P. J. E., 1972, ApJ, 178, 371
- Peters P. C., 1964, Physical Review, 136, 1224
- Peters P. C., Mathews J., 1963, Physical Review, 131, 435
- Porter E. K., Sesana A., 2010, ArXiv e-prints

Rezzolla L., 2009, *Classical and Quantum Gravity*, 26, 094023
Sutton A. D., Roberts T. P., Walton D. J., Gladstone J. C., Scott
A. E., 2012, ArXiv e-prints
Xu, S., et al. 2011, In preparation